ELSEVIER

Journal of Molecular Catalysis B: Enzymatic 8 (2000) 69–83

JOURNAL OF MOLECULAR CATALYSIS B: ENZYMATIC

Reaction products and intermediates of tryptophan tryptophylquinone enzymes

Victor L. Davidson *, Zhenyu Zhu

Department of Biochemistry, The University of Mississippi Medical Center, 2500 N. State Street, Jackson, MS 39216-4505, USA

Abstract

Methylamine dehydrogenase and aromatic amine dehydrogenase each possess the tryptophan tryptophylquinone (TTQ) cofactor which catalyzes the oxidative deamination of primary amines and transfer of substrate-derived electrons to type I copper proteins. The reaction steps and intermediates in the overall oxidation–reduction reactions catalyzed by these enzymes are described. An important feature of the reaction mechanism of TTQ-dependent amine dehydrogenases is that the product of the reductive half-reaction is the reduced aminoquinol in which the substrate-derived amino group is covalently incorporated into the reduced TTQ cofactor. This has been proven by use of ^{15}N NMR spectroscopy to monitor the fate of nitrogen from ^{15}N-labeled substrate. This intermediate is significant because the covalent incorporation of N into the reduced TTQ has profound effects on the rates of electron transfer and factors which regulate the electron transfer reactions from the reduced enzymes. Study of the oxidative half-reaction of methylamine dehydrogenase showed that incorporation of the substrate-derived amino group into TTQ caused this reaction to become gated by a proton transfer from the aminoquinol, and revealed an important role for monovalent cations in the regulation of this reaction step. Analysis of monovalent cation-induced perturbations of the absorption spectrum of TTQ-dependent enzymes has provided insight into the mechanism of cation–protein interactions.

Keywords: Methylamine dehydrogenase; Aromatic amine dehydrogenase; Tryptophan tryptophylquinone

1. Introduction

Tryptophan tryptophylquinone (TTQ, Fig. 1) [1] has been found thus far in two enzymes, methylamine dehydrogenase (MADH) and aromatic amine dehydrogenase (AADH). The covalently bound TTQ prosthetic group is formed by post-translational modification of two gene-encoded tryptophan residues of the host protein [2]. MADH has been isolated from several Gram-negative methylotrophic and autotrophic bacteria [reviewed in Refs. [3–5]]. AADH has been isolated from *Alcaligenes faecalis* [6,7]. These enzymes catalyze the oxidation of primary amines to their corre-

* Corresponding author. Tel.: +1-601-984-1515; fax: +1-601-984-1501; e-mail: vdavidson@biochem.umsmed.edu

1381-1177/00/$ - see front matter
PII: S1381-1177(99)00069-7

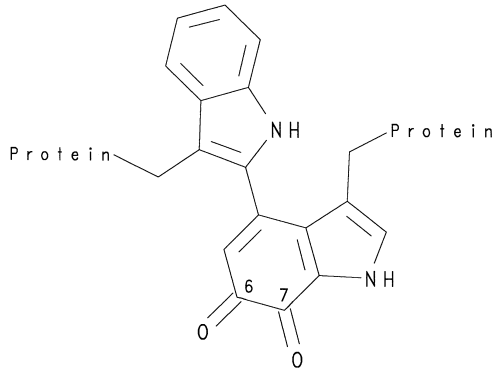

Fig. 1. The structure of TTQ. The C6 and C7 carbonyl carbons are labeled.

sponding aldehydes plus ammonia. The two electrons which are derived from this oxidation are subsequently transferred by the enzyme to some electron acceptor (Eq. (1)). The natural electron:

$$\text{R-CH}_2\text{NH}_3^+ + \text{H}_2\text{O} + 2\text{A}_{\text{ox}} \rightarrow \text{R-CHO} + \text{NH}_4^+ + 2\text{A}_{\text{red}} + 2\text{H}^+ \quad (1)$$

acceptor for MADH in most bacteria is a type I copper protein, amicyanin, which mediates electron transfer from MADH to *c*-type cytochromes [8,9]. The physiologic electron acceptor for AADH is another type I copper protein, azurin [10,11]. This paper will focus primarily on studies from this laboratory on AADH and the MADH from *Paracoccus denitrificans*.

2. Overall reaction mechanism

The overall oxidation–reduction reaction of MADH with methylamine and amicyanin may be divided into reductive (Eq. (2A)) and oxidative (Eq. (2B)) half-reactions. A detailed chemical:

$$\text{CH}_3\text{NH}_3^+ + \text{E-TTQ} \rightarrow \text{HCHO} + \text{E-TTQNH}_2 + 2\text{H}^+ \quad (2A)$$

$$\text{E-TTQNH}_2 + 2\text{A}_{\text{ox}} + \text{H}_2\text{O} \rightarrow \text{NH}_4^+ + 2\text{A}_{\text{red}} + \text{E-TTQ} \quad (2B)$$

reaction mechanism for the overall reaction, based on results of studies of the MADH from *P. denitrificans* is shown Fig. 2. The reductive and oxidative half-reactions require several steps that necessitate the presence of amino acid side chains capable of serving as either a general base or general acid. As many as 12 reaction steps involving general acids and bases (labeled B_1–B_{12} in Fig. 2) may be hypothesized. B_1 is required to bind and possibly deprotonate the substrate methylammonium to generate methylamine for nucleophilic attack of the C6 carbonyl carbon. B_2H facilitates the dehydration of the carbinolamine intermediate to form an imine. B_3 abstracts a proton from the methyl carbon which leads to reduction of the TTQ cofactor. This reaction step exhibits an anomalously large deuterium kinetic isotope effect [12] which suggests that the proton abstraction may involve quantum mechanical hydrogen tunneling. A large kinetic isotope effect of similar magnitude was also observed for the same reaction step in the mechanism of AADH [13]. B_4 coordinates and activates water for nucleophilic attack of the imine carbon. B_5 and B_6H facilitate cleavage of C–N bond and release of the formaldehyde product to yield the reduced aminoquinol reaction intermediate. The release of the aldehyde product appears to be the rate-determining step in

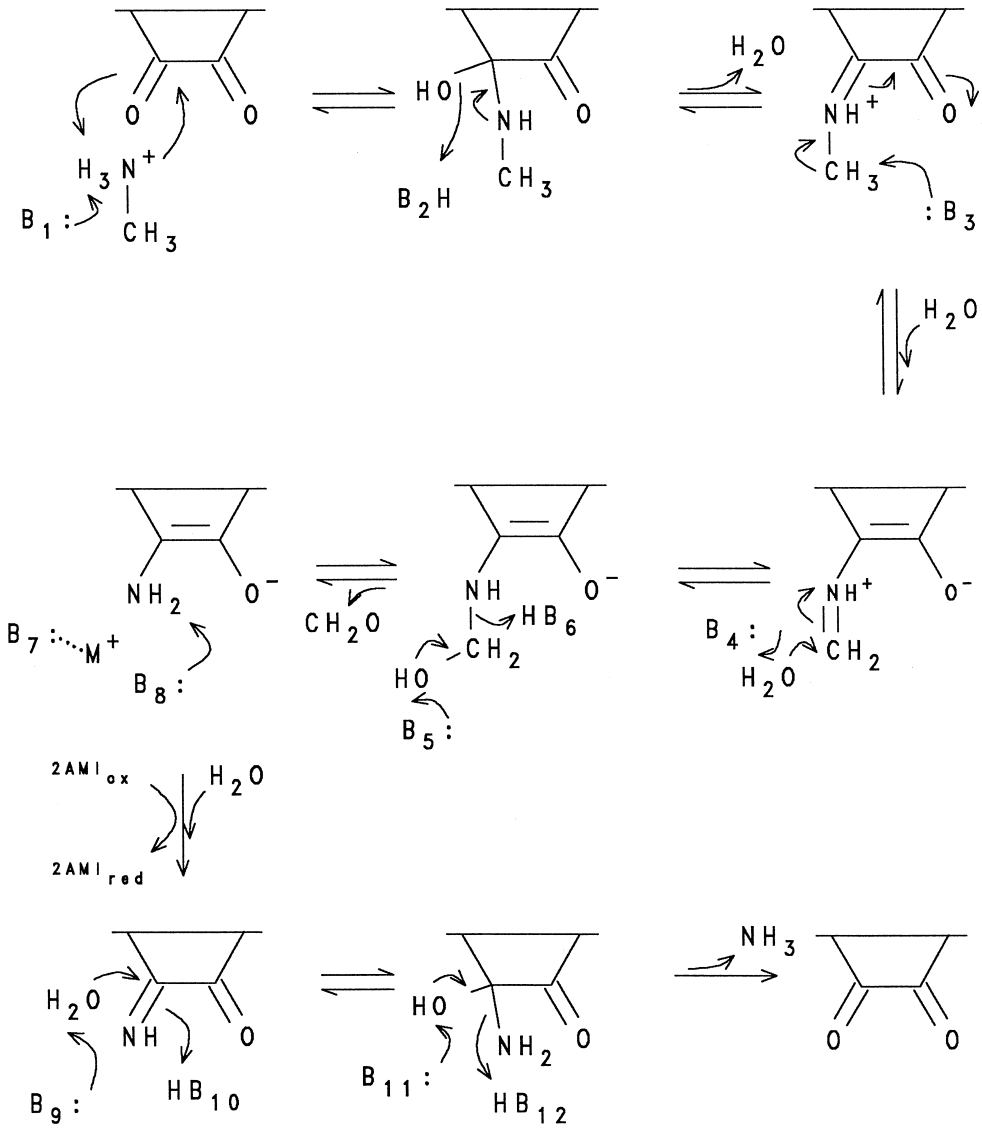

Fig. 2. The reaction mechanism of MADH. Reaction steps that have been proposed for the reductive and oxidative reactions are indicated. Only the quinone portion of TTQ is shown. B_1–B_{12} represent active-site residues which may serve as general acids or bases in the reaction steps. It is possible, and likely, that a single residue could perform multiple functions so that less than 12 such groups are needed in the active-site. The details of the mechanism are described in the text.

the reductive half-reaction [14]. Aldehyde release also appears to be the rate-determining step in the reductive half-reaction of AADH [15]. MADH is reoxidized in two one-electron transfers to amicyanin. The first electron transfer step requires the presence of a monovalent cation which is proposed to be bound to B_7 [16]. Another general base, B_8, is required to deprotonate the amino nitrogen to activate the intermediate for electron transfer [16,17]. B_9–B_{12} facilitate the hydrolysis of the iminoquinone after electron transfer to release the ammonia product and generate the oxidized quinol. While 12 roles for active-site residues have been proposed, it is possible that multiple roles

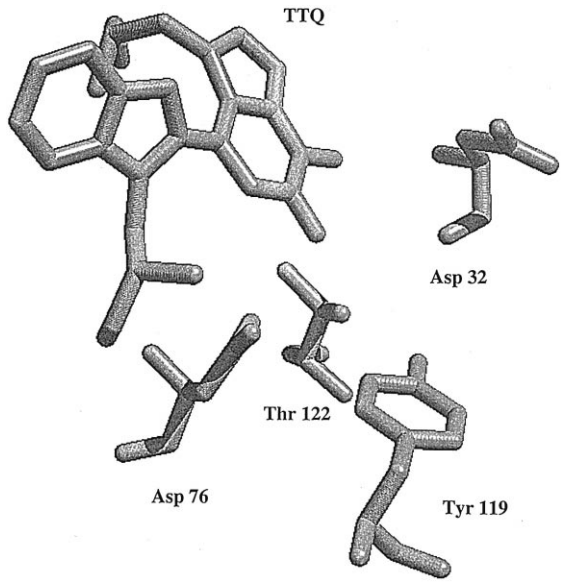

Fig. 3. The active-site of *P. denitrificans* MADH. A detailed description of the structure of MADH is presented in Ref. [20]. Coordinates are available in the Brookhaven data bank, entry 2BBK.

may be performed by a single residue so that less than 12 potentially active residues are likely to be sufficient to catalyze the complete oxidation–reduction reaction.

Asp76 has been previously proposed to be ''the'' active-site base in the reaction mechanism of MADH from *P. denitrificans* and *Thiobacillus versutus* based on its proximity to C6 of TTQ in the crystal structure [18,19]. This residue very likely does participate in some of the acid–base chemistry depicted in Fig. 2. However, other residues must also be involved. The high resolution crystal structure of MADH from *P. denitrificans* [20] reveals that the side chains of Thr122, Asp32 and Tyr119 are also in close enough proximity to C6 of TTQ to participate in the reaction (Fig. 3). The reaction mechanism requires that cation, water and substrate or product may all be required to be in the enzyme active-site at the same time. The presence of multiple solvent molecules in the active-site in the crystal structure [20] indicates that this is possible.

The ping-pong nature of the reaction mechanisms (Eqs. (2A) and (2B)) of MADH [21] and AADH [15] was originally inferred from the results of steady-state kinetic studies. Studies using ^{13}C and ^{15}N NMR spectroscopy have recently provided direct evidence for a ping-pong kinetic mechanism for both enzymes, and revealed points in the reaction mechanism at which the aldehyde and ammonia products are released. These results are summarized below.

3. Reductive half-reaction

To examine the fate of the substrate-derived carbon during the reductive half-reaction, the reactions of $^{13}CH_3NH_3Cl$ with AADH [22] and MADH [23] were studied in the absence of an oxidant (Table 1). $^{13}CH_3NH_3^+$ in the absence of enzyme exhibits a signal with a chemical shift of 27 ppm, in which the ^1H proton-coupled spectrum of this compound is split into a quartet, as is expected for an sp^3 hybridized carbon with three hydrogens bonded to it. Addition of AADH to this sample caused the appearance of a new signal exhibiting a chemical shift of 83 ppm, and the ^1H proton-coupled

Table 1
^{13}C and ^{15}N-NMR chemical shifts of enzyme reaction products and intermediates and reference compounds. Chemical shifts are referenced to liquid $NH_3 = 0$ for ^{15}N and tetramethylsilane = 0 for ^{13}C. Data are taken from Refs. [22–25]

Compound	Chemical shift (ppm)	
	^{15}N	^{13}C
$^{13}CH_3\,^{15}NH_3^+$	35	27
$^{15}NH_4^+$	35	–
^{13}CHO	–	220
$^{13}CH_2(OH)$	–	83
$C_6H_5\,^{15}NH_2$	–	60–70
Products of reaction of	–	83
MADH + methylamine	35	–
Products of reaction of	–	83
AADH + methylamine	35	–
MADH TTQ-^{15}N-aminoquinol	54	–
AADH TTQ-^{15}N-aminoquinol	61	–

spectrum of this new was split into a triplet [22]. This indicates that this carbon has only two hydrogens bonded to it, as would be expected for the oxidized aldehyde product. Neat formaldehyde ($^{13}CH_2O$)) exhibits a chemical shift at 220 ppm [24] which is far upfield of this signal. However, 1,1-formalin-diol ($^{13}CH_2(OH)_2$), which is the hydrate of formaldehyde that is formed on reaction with water, does exhibit a chemical shift at 83 ppm [24,25]. These results indicated that the aldehyde product was formed and released from AADH in the absence of an oxidant. Essentially, identical results were obtained when labeled substrate was incubated with MADH [23] (Table 1). These results confirm the previously proposed ping-pong kinetic mechanisms for MADH [21] and AADH [15] in which the aldehyde product is released prior to reoxidation by the electron acceptor.

A critical question is whether the ammonia product is also released at this point. Proof that the substrate-derived nitrogen forms a stable covalent adduct with the TTQ cofactors of MADH and AADH, and that ammonia is released only after the enzyme is reoxidized was obtained by ^{15}N NMR spectroscopy [22,25] (Fig. 4). The ^{15}N NMR spectrum of $CH_3\,^{15}NH_3Cl$ in the absence of enzyme exhibits a single feature at 35 ppm (Fig. 4A). When $CH_3\,^{15}NH_3Cl$ was incubated with AADH, two signals were observed in the ^{15}N NMR spectrum (Fig. 4B). The signal at 35 ppm is characteristic of the unreacted excess $CH_3\,^{15}NH_3^+$. The second signal at 61 ppm is the result of the reaction of substrate with AADH. This chemical shift is in the range seen for N which is covalently bonded to an aromatic system (e.g., aniline), as would be expected if the substrate-derived N were covalently bound to TTQ [22] (Table 1). Similar results were obtained when MADH was incubated with $CH_3\,^{15}NH_3Cl$ [25] (Fig. 5 and Table 1). One important difference was that the substrate-derived N on the aminoquinol intermediate exhibited a chemical shift at 54 ppm. This likely reflects differences in the active-site environments of TTQ in MADH and AADH. The aminoquinol of MADH was also much more stable against oxygen than the aminoquinol of AADH [22]. With MADH, it was possible to dialyze away excess unreacted methylamine and retain the signal of the protein-bound aminoquinol at 54 ppm (Fig. 5B). After addition of an oxidant to the MADH aminoquinol, the 54 ppm signal disappeared and a single signal was observed at 35 ppm. This new signal is attributable to the free ammonium product which possesses the substrate-derived N. As seen in Fig. 5C, the signal from $^{15}NH_4Cl$ exactly overlays that of the product of the oxidation of the MADH aminoquinol.

The covalent adduct formation that gives rise to the change in the ^{15}N chemical shifts may also be concluded from relaxation studies. Large molecules, such as proteins, tumble relatively slowly in

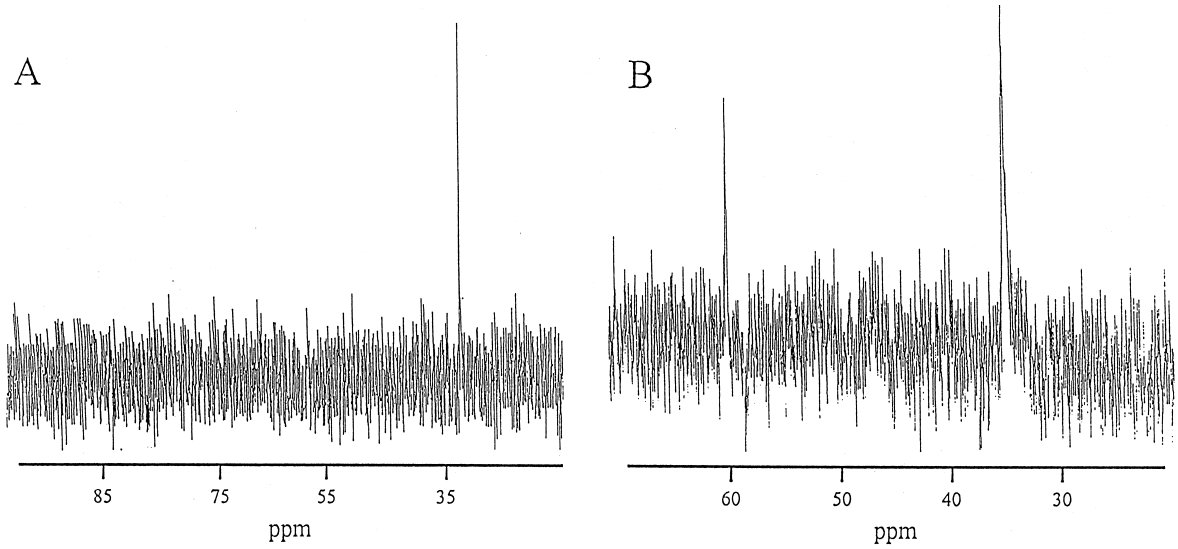

Fig. 4. ^{15}N NMR spectra of $CH_3{}^{15}NH_3Cl$ in the presence and absence of AADH. (A) The ^{1}H-decoupled ^{15}N NMR spectrum of $CH_3{}^{15}NH_3Cl$ in the absence of AADH. (B) The ^{1}H-decoupled ^{15}N NMR spectrum of a mixture of AADH with excess $CH_3{}^{15}NH_3Cl$. No oxidant was added to these samples. This figure was adapted from Ref. [22]. Experimental details may be found in that reference.

solution because of their size and will relax much more efficiently than small rapidly tumbling molecules such as $CH_3NH_3^+$ and NH_4^+. If ^{15}N forms a covalent adduct with MADH, we will observe a significant decrease in relaxation time compared to free $CH_3{}^{15}NH_3^+$. In these studies [22,25], the signals at 54 and 61 ppm, for MADH and AADH, respectively, accumulated optimally with a short pulse delay, whereas the signals at 35 ppm accumulated optimally with a long pulse delay. That these species exhibit such different relaxation characteristics is consistent with the signals at 54 and 61 ppm, which appear optimally with short pulse delay, deriving from the covalent aminoquinol reaction intermediate, while those at 35 ppm are derived from small solutes.

^{13}C and ^{15}N NMR studies of the reactions of MADH and AADH demonstrate that the products of the reductive half-reaction are an equivalent of formaldehyde hydrate and a reduced aminoquinol form of TTQ which contains covalently bound substrate-derived N (Table 1). These data are consistent with the ping-pong kinetic mechanism and aminotransferase-type chemical reaction mechanism. It should be noted that similar conclusions were obtained from results of studies of amine oxidation by a TTQ model compound [26]. These results also demonstrate the utility of ^{13}C and ^{15}N NMR spectroscopy for detecting and characterizing intermediates in enzyme-catalyzed reactions.

4. Oxidative half-reaction

While NMR studies have established that a stable aminoquinol is the product of the reductive half-reaction of TTQ enzymes, these results do not distinguish whether the ammonia product is released after the first or the second electron transfer during the oxidative half-reaction. In other words, is the intermediate in the two-step oxidation of MADH by amicyanin a semiquinone or an aminosemiquinone (*N*-semiquinone) with substrate-derived N still bonded to TTQ? Proof that the MADH semiquinone intermediate retains the substrate-derived N has been obtained from transient kinetic studies and spectroscopic studies which are summarized below.

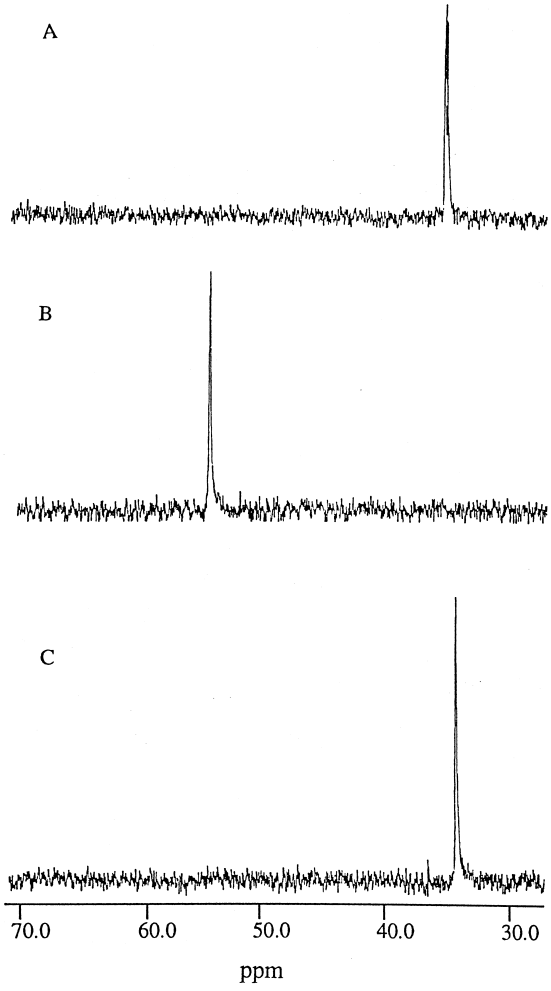

Fig. 5. ^{15}N NMR spectra depicting the fate of substrate-derived ^{15}N during the catalytic cycle of MADH. (A) The ^{1}H-decoupled ^{15}N NMR spectrum of $CH_3{}^{15}NH_3Cl$ in the absence of MADH. (B) The ^{1}H-decoupled ^{15}N NMR spectrum of MADH after reaction with excess $CH_3{}^{15}NH_3Cl$ in the absence of added oxidant and subsequent dialysis. (C) The ^{1}H-decoupled ^{15}N NMR spectrum of the sample in B after oxidation by addition of excess phenazine ethosulfate, plus addition of $^{15}NH_4Cl$. This figure was adapted from Ref. [25]. Experimental details may be found in that reference.

Rapid-scanning stopped-flow spectroscopy and global kinetic analysis were used to demonstrate that *N*-semiquinone is a true physiologic reaction intermediate which accumulates during the two sequential one-electron oxidations of the substrate-reduced aminoquinol MADH by amicyanin [27]. The differences in the relative reaction rates for the first and second electron transfer reactions from the dithionite-generated quinol and substrate-reduced aminoquinol are clearly seen in Fig. 6. No intermediate was observed with the dithionite-reduced enzyme because the rate of the second oxidation was orders of magnitude faster than the rate of the first oxidation (Fig. 6A, Table 2). The intermediate is observed during the reaction of the aminoquinol (Fig. 6B) since the rates of the first and second oxidation steps are more similar. The rate of the second one-electron transfer from substrate-reduced MADH to amicyanin was also shown to be comparable to the rate of reaction of an

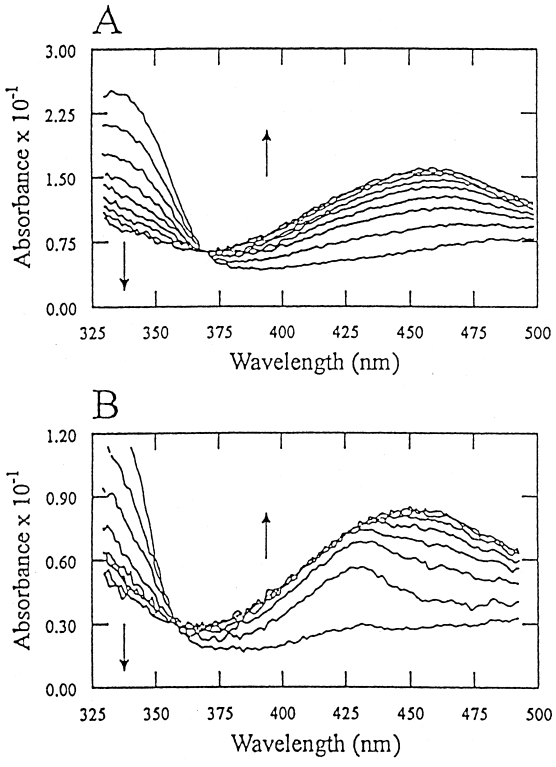

Fig. 6. Rapid-scanning spectroscopic analysis of the complete oxidation of MADH by amicyanin. (A) The reaction of 2 μM dithionite-reduced (*O*-quinol) MADH with 50 μM amicyanin at 25°C in 10 mM potassium phosphate buffer, pH 7.5. The arrows indicate the directions of the spectral changes with time. The spectra that are displayed were recorded 30 ms apart. (B) The reaction of 2 μM substrate-reduced aminoquinol MADH with 50 μM amicyanin. Reaction conditions were identical to those in A. The spectra that are displayed were recorded 20 ms apart. This figure was adapted from Ref. [27]. Experimental details may be found in that reference.

N-semiquinone form of MADH which was generated in vitro. This *N*-semiquinone form can be generated by comproportionation of the fully oxidized quinone and aminoquinol forms of MADH at alkaline pH [28]. The presence of the substrate-derived nitrogen in this N-semiquinone was demonstrated by electron spin echo envelope modulation (ESEEM) spectroscopy of *N*-semiquinones which were prepared with unlabeled and ^{15}N-labeled methylamine [29]. These comparative studies demonstrated that the intermediate which accumulates during the two-step oxidation of aminoquinol MADH by amicyanin is kinetically identical to the *N*-semiquinone which is generated by comproportionation, and possesses a substrate-derived nitrogen.

An alternative explanation for the results described above is that the *N*-semiquinone does not exist as a reaction intermediate but that properties attributed to the *N*-semiquinone may be due to the influence of ammonia which is non-covalently bound at the active-site in close proximity to the C6 oxygen of the *O*-semiquinone species [30]. To test this hypothesis, the reactions of the dithionite-reduced forms of MADH with amicyanin were performed in the presence of 200 mM ammonium chloride. The presence of this high concentration of ammonia (well above the K_d value) had no effect on the reaction. As reported [27], no intermediate accumulates during the reaction of the quinol with amicyanin in the presence of ammonia. As in Fig. 6A, the reaction of the semiquinone is much faster than the reaction of the quinol. The presence of excess ammonia, therefore, does not mimic the *N*-semiquinone results and the kinetic behavior attributed to being that of the covalent *N*-semi-

Table 2
Rate-limiting steps for electron transfer reactions from different redox forms of MADH to amicyanin. Values for the rate constants are taken from Ref. [26]. Reaction conditions are 10 mM potassium phosphate, pH 7.5, plus 0.2 M KCl at 25°C

MADH redox form	Rate-limiting reaction step	Rate constant (s^{-1})
O-quinol MADH	electron transfer	11
O-semiquinone MADH	electron transfer	> 500
N-quinol MADH	proton transfer	160
N-semiquinone MADH	electron transfer	70

quinone, cannot be due instead to the effect of non-covalently bound ammonia on the *O*-semiquinone. These results clearly demonstrate that the substrate-derived N is not released from TTQ until after the second one-electron oxidation step.

The ability to generate stable reduced and semiquinone forms of MADH by reaction with either dithionite or substrate has allowed us to study the electron transfer reactions from four different redox forms of MADH to amicyanin (Table 2). Each reaction exhibits a different rate constant. Analysis of the free energy dependence of the dithionite-generated MADH forms [31] and the temperature dependencies of the dithionite-reduced [32], substrate-reduced [17] and *N*-semiquinone [33] forms yielded thermodynamic and Marcus parameters for each electron transfer reaction. These results indicate that the differences in rates for the reactions of dithionite-reduced *O*-quinol and *O*-semiquinone, and *N*-semiquinone with amicyanin are due to differences in the redox potentials of the different MADH forms. Marcus theory [34] describes the dependence of electron transfer rate on ΔG°. The ΔE_{m} values for the oxidation by amicyanin of the different MADH redox forms have been estimated to be: *O*-quinol = +31 mV [31]; *O*-semiquinone = +207 mV [31]; and *N*-semiquinone + 166 mV [33]. The electron transfer reactions of these three redox forms with amicyanin exhibit a variation in rate with free energy that is predicted by Marcus theory [31,33]. Furthermore, analysis of the temperature dependence of the electron transfer rates to amicyanin from *O*-quinol MADH [32] and *N*-semiquinone MADH [33] yielded a calculated electron transfer distance that closely matched the distance between TTQ and copper which is seen in the crystal structures of complexes of these proteins [35,36]. In contrast, analysis of the temperature dependence of the rate of the electron transfer reaction from the substrate-reduced aminoquinol MADH to amicyanin indicated that this reaction was gated [17]. That analysis yielded a value for the electronic coupling which was well in excess of the nonadiabatic limit and predicted a negative distance. Such results are indicative that it is inappropriate to analyze the reaction by Marcus theory, and diagnostic of a redox reaction that is gated (i.e., rate-limited) by an adiabatic, non-electron transfer event [37]. For the reaction of the *N*-quinol, that rate-limiting step was shown to be the transfer of a solvent exchangeable proton [17]. This rate-limiting proton transfer step was dependent on pH and the concentration of monovalent cations [16], and exhibited a primary deuterium kinetic solvent isotope effect [17]. These results were explained by a model in which the effect of the cation is to stabilize a negatively charged reaction intermediate that is formed during the deprotonation of the substrate-derived N of the aminoquinol. It is from this unstable intermediate that the relatively rapid ET to the copper of amicyanin occurs.

The proposed mechanism for the cation and pH dependent deprotonation of *N*-quinol TTQ that gates electron transfer from MADH to amicyanin is summarized in Fig. 7. In this model, binding of a monovalent cation (M^{+}) plays an essential role in deprotonating *N*-quinol TTQ and activating it for rapid electron transfer to amicyanin. For M^{+} to bind at the active-site requires that an active-site base (X_1, B_7 in Fig. 2) provides a ligand in close proximity the *N*-quinol nitrogen. The pH dependence of the reaction reflects the need to deprotonate this active-site residue so that it may bind M^{+}. After

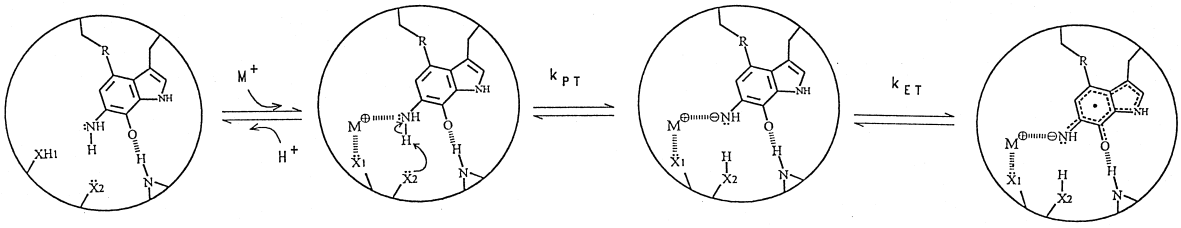

Fig. 7. A model for monovalent cation-dependent electron transfer from aminoquinol MADH to amicyanin. Dashed lines indicate electrostatic and H-bonding interactions. X_1 and X_2 are ionizable active-site residues. This electron transfer reaction is gated because the rate of the prerequisite proton transfer reaction (k_{PT}) is slower than the rate of the electron transfer reaction (k_{ET}). Details of this mechanism are presented in the text.

binding M^+, TTQ-bound NH_2 is deprotonated by another active-site residue (X_2, B_8 in Fig. 2). M^+ may interact with the NH_2 group via the lone pair of electrons on N and weaken the N–H bond to activate it for abstraction, stabilize the formation of a transition-state intermediate with partial negative charge, and stabilize the anionic product following deprotonation. After this rate-limiting deprotonation, rapid electron transfer occurs. The anionic radical product may then either be reprotonated by X_2H to yield an aminosemiquinone or rearrange to an iminosemiquinone. In the absence of M^+, deprotonation of the substrate-derived N is much less favorable. This explains the large rate enhancement by M^+. This gating phenomenon is only observed with the aminoquinol form of MADH. This demonstrates that the covalent incorporation of substrate-derived N into reduced TTQ during the reductive half-reaction has a profound effect on the rates and regulation of the electron transfer reaction from MADH to amicyanin (see Table 2).

5. Effects of monovalent cations on spectral properties

Monovalent cations and pH influence the UV–visible absorption spectra of both MADH [38] and AADH [39]. To determine the molecular basis for these spectral perturbations, we performed a

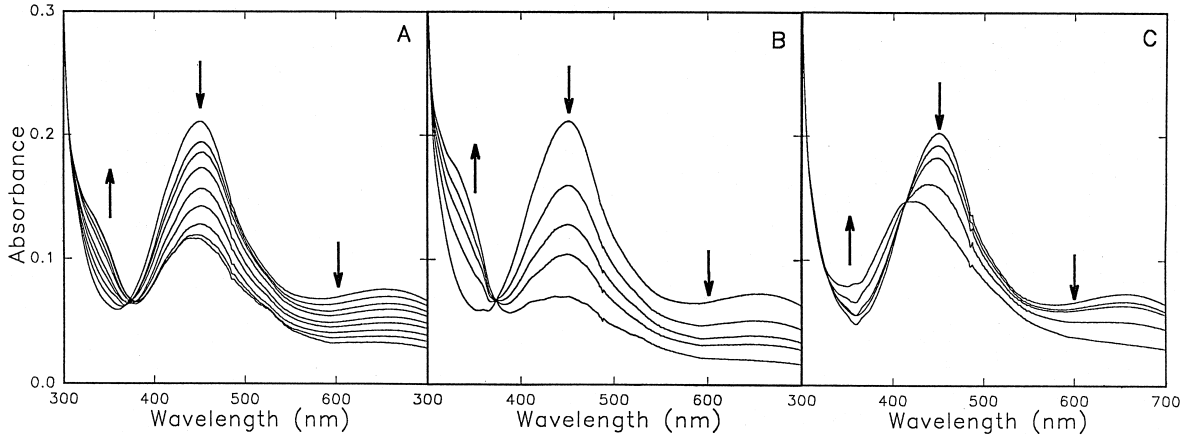

Fig. 8. Effects of monovalent cations on the absorption spectrum of oxidized AADH. All titrations were performed in 10 mM BisTris propane buffer, pH 9.0, at 25°C. Each spectrum is normalized so that A_{280} was equal to 1.0. The arrows indicate the directions of the spectral changes. (A) NaCl was present at 0, 50, 100, 190, 370, 690, 1200, 1950, and 2800 mM. (B) KCl was present at 0, 40, 155, 570, and 1700 mM. (C) NH_4^+/NH_3 was present at 0, 5, 10, 40, 80, and 155 mM.

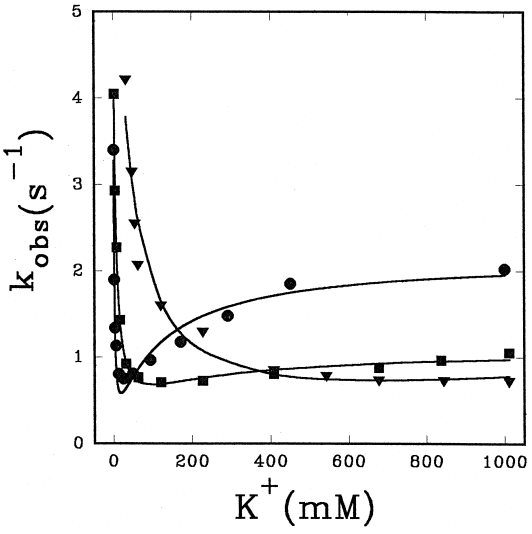

Fig. 9. Effects of pH and K^+ concentration on the rate of cation-induced spectral changes. All stopped-flow experiments were performed in 10 mM BisTris propane buffer, at the indicated pH, at 25°C. K^+ concentrations are the concentration after mixing. The solid lines are fits of the data to Eq. (3) using the value for K_a which was obtained from analysis using Eq. (4). (▼) pH 8.0; (■) pH 9.0; (●) pH 10.0.

detailed spectroscopic and kinetic analysis of the cation-induced changes in the spectrum of AADH [39]. Little spectral perturbation was observed when pH was varied in the absence of monovalent cations. The addition of alkali metal monovalent cations (i.e., K^+, Na^+, Li^+, Rb^+, Cs^+) to oxidized AADH caused significant changes in its absorption spectrum (Fig. 8). The apparent K_d for each cation, determined from titrations of the spectral perturbation, decreased with increasing pH. Transient kinetic studies involving rapid mixing of AADH with cations, and pH jump, revealed that the rate of the cation-induced spectral changes initially decreased with increasing cation concentration to a minimum value, then increased with increasing cation concentration (Fig. 9). A kinetic model (discussed later) was developed to fit these data, determine the true pH-independent K_d values for K^+ and Na^+, and explain the pH-dependence of the apparent K_d.

A chemical reaction mechanism that is based on the kinetic data is presented in Fig. 10. It is proposed that the metallic monovalent cation facilitates the chemical modification of the TTQ prosthetic group to form a hydroxide adduct which gives rise to the spectral change. It is proposed that the C6 position of TTQ is the site of reaction. This has been shown to be the reactive carbonyl of TTQ in MADH [19] and of TTQ model compounds [40]. One active-site residue X_1 (also X_1 in Fig. 7

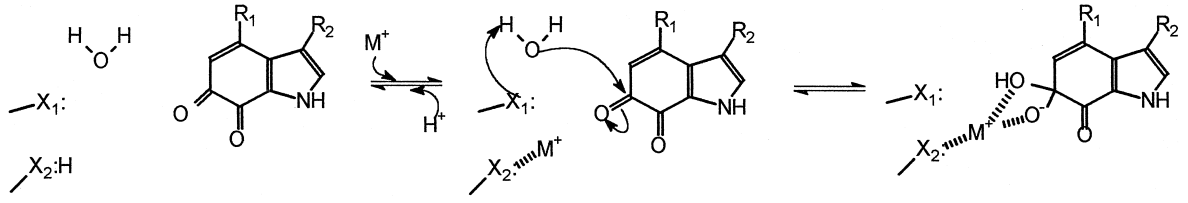

Fig. 10. Proposed chemical reaction mechanism for the cation-induced spectral perturbations of TTQ-dependent enzymes. X_1 and X_2 represent amino acid residues at the active-site. X_1 is a general base which activates water for nucleophilic attack of the C6 carbonyl carbon of TTQ. X_2 serves as a ligand for the monovalent cation (M^+) when it is unprotonated. This allows alkali metallic cations to facilitate hydration of TTQ to give rise to a spectral change. R_1 represents the second indol ring of TTQ and R_2 is the polypeptide chain to which TTQ is linked at that point.

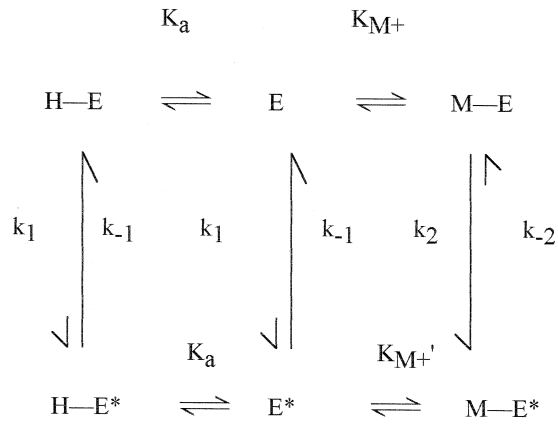

Scheme 1.

and B_7 in Fig. 2) serves as a ligand for the monovalent cation (M^+) when it is unprotonated. The other X_2 serves as a general base which activates water for nucleophilic attack of the C6 carbonyl carbon of TTQ. The formation of a hydroxide adduct of TTQ in MADH at high pH has previously been demonstrated by resonance Raman spectroscopy [41].

A kinetic model that describes the effects of metallic monovalent cations and pH on the spectral properties of AADH is given in Scheme 1. This model accounts for the observed dependencies of the rates and extents of spectral perturbations on specific cations and $[H^+]$. According to this model, the spectral perturbations are caused not simply by cation binding, but by conversion of E to another enzyme form $[E^*]$ with distinct spectral properties. The presence of the metallic cation (M^+) stabilizes E^* relative to E. E^* could represent a different conformation of the enzyme or, as proposed in Fig. 10, enzyme with a modified cofactor. This model assumes that some active-site group with a dissociable proton, when unprotonated, serves as a ligand for the metallic cation (M). M–E represents the quinone form with a metallic cation bound at the active-site. In H–E this active-site group is protonated and, therefore, unable to serve as a ligand for M. E represents enzyme with this group unprotonated but without M bound at the active-site. K_a is the dissociation constant for the H–E proton. K_{M+} is the dissociation constant for the M–E complex. Since this constant may be different for E and E^*, it is designated K'_{M+} for the latter. A rate equation for Scheme 1 is given in Eq. (3).

$$k_{obs} = \frac{k_2[M]}{K_{M+}(1 + [H^+]/K_a) + [M]} + \frac{k_{-1}K'_{M+}(1 + [H^+]/K_a)}{K'_{M+}(1 + [H^+]/K_a) + [M]} \tag{3}$$

This model assumes that the binding and dissociation of M^+ and H^+ to all enzyme forms are in rapid equilibrium, that all E forms are spectroscopically indistinguishable from each other, and that all E^* forms are spectroscopically indistinguishable from each other. To simplify the rate equation, it was also assumed that $k_{-1} \gg k_1$ and $k_2 \gg k_{-2}$. The value of K_a was obtained by fitting the titration data at different values of pH for each M^+ to Eq. (4), which is derived in [39].

$$A/A_0 = \frac{1 + \{(1/K_{M+} + \alpha K_1/K'_{M+})/(1 + \alpha K_1)\}\{[M]/(1 + [H^+]/K_a)\}}{1 + \{(1/K_{M+} + \alpha K_1/K_{M+})/(1 + K_1)\}\{[M]/(1 + [H^+]/K_a)\}} \tag{4}$$

The term α is the ratio of the extinction coefficients for E^*/E and K_1 is k_1/k_{-1} in Scheme 1. As seen in Fig. 9, the experimental data can be fit quite well to this model. This justifies the assumptions concerning the relative magnitudes of rate constants that were used to simplify Eq. (3). It is also clear

Table 3
Apparent dissociation constants for metallic monovalent cation binding to TTQ enzymes. Apparent K_d values were obtained by analyzing the data from titrations such as those in Fig. 8 according to $\Delta A = \Delta A_{max}[M^+]/(K_d + M^+)$. Values for AADH were previously reported in Ref. [39]. Values for MADH are for the *P. denitrificans* enzyme and have not been previously reported

Cation	Apparent K_d at pH 9.0 (mM)	
	AADH	MADH
Na^+	360	20
K^+	140	80
Li^+	620	20
Rb^+	220	30

from this model that K_d values for TTQ enzymes that are determined from fits of static spectral titrations are not true K_d values, but apparent K_d values that describe the overall equilibrium shown in Scheme 1. Apparent K_d values for cation binding to AADH at pH 9.0 are given in Table 3. The true dissociation constants for Na^+ and K^+ which were determined for AADH using Eq. (4) are for K^+, $K_{M+} = 34$ mM and $K'_{M+} = 0.3$ mM, and for Na^+, $K_{M+} = 81$ mM and $K'_{M+} = 4.0$ mM. For AADH, the titration data at different values of pH for Na^+ and K^+ yielded identical values of $K_a = 5.0 \pm 1.0 \times 10^{-11}$ M ($pK_a = 10.3$) [39].

Addition of NH_4^+/NH_3 to AADH caused changes in its absorption spectrum which were much different than those caused by addition of the metallic monovalent cations (Fig. 8). The kinetics of the reaction induced by addition of NH_4^+/NH_3 were also different, exhibiting simple saturation kinetics [39]. One explanation for the NH_4^+/NH_3 induced spectral change is that it results from nucleophilic addition of the unprotonated NH_3 to TTQ in AADH [39].

While the effects of monovalent cations on the absorption spectra of MADH [38,42] and AADH [39] are similar, there are some significant differences. Comparison of apparent K_d values at pH 9.0 suggest that monovalent cations have a greater affinity for MADH than AADH (Table 3). Differences in the reactions of MADH and AADH with NH_4^+/NH_3 are also evident. A red shift in the absorption spectrum of MADH is observed [38], whereas with AADH a blue shift is observed (Fig. 8) [39]. Subtle differences are also observed between MADH from different sources. With MADH from *P. denitrificans*, the apparent K_d at pH 9.0 for K^+ is greater than that for Na^+ [38]. However, with MADH from bacterium W3A1, the apparent K_d for Na^+ is greater than that for K^+ [42]. These data suggest that while these enzymes each have the same TTQ cofactor, differences in the active-site environment may exist that affect the specificity of the cation binding process.

It is very likely that the metallic monovalent cation binding site described in Fig. 10 is the same as that described in Fig. 7, which is necessary to activate the aminoquinol form of the enzyme for electron transfer. A monovalent cation positioned at that site could also stabilize the carbanionic intermediate which is formed during the reductive half-reaction of TTQ (Fig. 2). Thus, while the mechanism proposed in Fig. 10 may not be of physiologic relevance, the pH- and cation-induced spectral perturbations of TTQ enzymes do provide a nice handle for examining important cation–protein interactions which occur at the active-sites of these enzymes.

6. Conclusions

TTQ enzymes may serve as models for the study of several important biologic phenomena. As seen in Figs. 2 and 7, several types of reactions of fundamental importance to enzymology have been

studied with TTQ enzymes. These include nucleophilic addition, hydrolysis reactions, proton transfer reactions from carbon, and proton transfer reactions between heteroatoms. Since TTQ enzymes use other redox proteins as electron acceptors in their oxidative half-reactions, they are also valuable systems in which to study the factors which stabilize protein–protein interactions [43] and the mechanisms of long range electron transfer through proteins [32]. Continued study of the structure and function of TTQ enzymes will continue to enhance our understanding of mechanisms of enzymatic catalysis and protein electron transfer reactions.

Acknowledgements

Work performed in this laboratory has been supported by NIH grant GM-41574. We acknowledge the contributions of the following members of this laboratory and collaborative researchers to the previously published work which was summarized in this review: Limei Jones, M. Elizabeth Graichen, Harold B. Brooks, Young-Lan Hyun, G. Reid Bishop, F. Scott Mathews (Washington University), and Rickey P. Hicks (Mississippi State University).

References

[1] W.S. McIntire, D.E. Wemmer, A.Y. Christoserdov, M.E. Lidstrom, Science 252 (1991) 817.
[2] A.Y. Chistoserdov, Y.D. Tsygankov, M.E. Lidstrom, Biochem. Biophys. Res. Commun. 172 (1990) 211.
[3] V.L. Davidson, in: V.L. Davidson (Ed.), Principles and Applications of Quinoproteins, Marcel Dekker, New York, 1993, pp. 73–95.
[4] J.P. Klinman, D. Mu, Annu. Rev. Biochem. 63 (1994) 299.
[5] J.A. Duine, Eur. J. Biochem. 200 (1991) 271.
[6] M. Iwaki, T. Yagi, K. Horiike, Y. Saeki, T. Ushijima, M. Nozaki, Arch. Biochem. Biophys. 220 (1983) 253.
[7] S. Govindaraj, E. Eisenstein, L.H. Jones, J. Sanders-Loehr, A.Y. Chistoserdov, V.L. Davidson, S.L. Edwards, J. Bacteriol. 176 (1994) 2922.
[8] M. Husain, V.L. Davidson, J. Biol. Chem. 260 (1985) 14626.
[9] R. Durley, L. Chen, L.W. Lim, F.S. Mathews, V.L. Davidson, Protein Sci. 2 (1993) 739.
[10] S.L. Edwards, V.L. Davidson, Y.-L. Hyun, P.T. Wingfield, J. Biol. Chem. 270 (1995) 4293.
[11] Y.-L. Hyun, V.L. Davidson, Biochemistry 34 (1995) 12249.
[12] H.B. Brooks, L.H. Jones, V.L. Davidson, Biochemistry 32 (1993) 2725.
[13] Y.-L. Hyun, V.L. Davidson, Biochim. Biophys. Acta 1251 (1995) 198.
[14] V.L. Davidson, M.E. Graichen, L.H. Jones, Biochem. J. 308 (1995) 487.
[15] Y.-L. Hyun, V.L. Davidson, Biochemistry 34 (1995) 816.
[16] G.R. Bishop, V.L. Davidson, Biochemistry 36 (1997) 12950.
[17] G.R. Bishop, V.L. Davidson, Biochemistry 34 (1995) 12082.
[18] L. Chen, F.S. Mathews, V.L. Davidson, E. Huizinga, F.M.D. Vellieux, J.A. Duine, W.G.J. Hol, FEBS Lett. 287 (1991) 163.
[19] E.G. Huizinga, B.A.M. van Zanten, J.A. Duine, J.A. Jongejan, F. Huitema, K.S. Wilson, W.G.J. Hol, Biochemistry 31 (1992) 9789.
[20] L. Chen, M. Dol, R.C.E. Durley, A.Y. Chistoserdov, M.E. Lidstrom, V.L. Davidson, F.S. Mathews, J. Mol. Biol. 276 (1998) 131.
[21] V.L. Davidson, Biochem. J. 261 (1989) 107.
[22] G.R. Bishop, Z. Zhu, T.L. Whitehead, R.T. Hicks and, V.L. Davidson, Biochem. J. 330 (1997) 1159.
[23] G.R. Bishop, R.T. Hicks, V.L. Davidson, 1997, unpublished results.
[24] G.C. Levey, G.L. Nelson, Carbon-13 Nuclear Magnetic Resonance for Organic Chemists, Wiley, New York, 1972.
[25] G.R. Bishop, E.J. Valente, T.L. Whitehead, K.L. Brown, R.T. Hicks, V.L. Davidson, J. Am. Chem. Soc. 118 (1996) 12868.
[26] S. Itoh, N. Takada, T. Ando, S. Haranou, X. Huang, Y. Uenoyama, Y. Oshiro, M. Komatsu, S. Fukuzumi, J. Org. Chem. 62 (1997) 5898.
[27] G.R. Bishop, H.B. Brooks, V.L. Davidson, Biochemistry 35 (1996) 8948.
[28] V.L. Davidson, L.H. Jones, M.A. Kumar, Biochemistry 29 (1990) 10786.
[29] K. Warncke, H.B. Brooks, G.T. Babcock, V.L. Davidson, J.L. McCracken, J. Am. Chem. Soc. 115 (1993) 6464.
[30] A.C.F. Gorren, S. de Vries, J.A. Duine, Biochemistry 34 (1995) 9748.
[31] H.B. Brooks, V.L. Davidson, J. Am. Chem. Soc. 116 (1994) 11201.

[32] H.B. Brooks, V.L. Davidson, Biochemistry 33 (1994) 5696.
[33] G.R. Bishop, V.L. Davidson, Biochemistry 37 (1998) 11026.
[34] R.A. Marcus, N. Sutin, Biochim. Biophys. Acta 811 (1985) 265.
[35] L. Chen, R. Durley, B.J. Poloks, K. Hamada, Z. Chen, F.S. Mathews, V.L. Davidson, Y. Satow, E. Huizinga, F.M.D. Vellieux, W.G.J. Hol, Biochemistry 31 (1992) 4959.
[36] L. Chen, R. Durley, F.S. Mathews, V.L. Davidson, Science 264 (1994) 86.
[37] V.L. Davidson, Biochemistry 35 (1996) 14035.
[38] V. Kuusk, W.S. McIntire, J. Biol. Chem. 269 (1994) 26136.
[39] Z. Zhu, V.L. Davidson, Biochem. J. 329 (1997) 175.
[40] S. Itoh, N. Takada, S. Haranou, T. Ando, M. Komatsu, Y. Oshiro, S. Fukuzumi, J. Am. Chem. Soc. 117 (1995) 1485.
[41] G. Backes, V.L. Davidson, F. Huitema, J.A. Duine, J. Sanders-Loehr, Biochemistry 30 (1991) 9201.
[42] Z. Zhu, V.L. Davidson, 1997, unpublished results.
[43] V.L. Davidson, L.H. Jones, M.E. Graichen, F.S. Mathews, J.P. Hosler, Biochemistry 36 (1997) 12733.